A Convergence Test of the Full-potential Linearized Augmented Plane Wave (FLAPW) Method: Ferromagnetic Bulk BCC Fe

Seung-Woo Seo[1], You Young Song[1], Gul Rahman[1], In Gee Kim[1]*, M. Weinert[2], and A. J. Freeman[3]

[1]*Graduate Institute of Ferrous Technology, Pohang University of Science and Technology, Pohang 790-784, Korea*
[2]*Department of Physics, University of Wisconsin-Milwaukee, PO BOX 413, Milwaukee, WI 53201, U.S.A.*
[3]*Department of Physics and Astronomy, Northwestern University, Evanston, IL 60208, U.S.A.*

The convergence behavior of the all-electron full-potential linearized augmented plane-wave (FLAPW) method with the explicit orthogonalization (XO) scheme is tested on ferromagnetic bulk body-centered-cubic Fe. Applying a commonly used criterion relating the plane-wave and angular momentum cutoffs, $l_{max} = R_{MT}K_{max}$, where R_{MT} is the muffin-tin (MT) sphere radius and K_{max} is the plane-wave cutoff for the basis – the total energy is converged and stable for $K_{max}R_{MT} = 10$. The total energy convergence dependence on the star-function cutoff, G_{max}, is minimal and so a G_{max} of $3K_{max}$ or a large enough G_{max} is a reasonable choice. We demonstrate that the convergence with respect to l_{max} or a fixed large enough G_{max} and K_{max} are independent, and that K_{max} provides a better measure of the convergence than $R_{MT}K_{max}$. The dependence of the total energy on R_{MT} is shown to be small if the core states are treated equivalently, and that the XO scheme is able to treat systems with significantly smaller R_{MT} than the standard LAPW method. For converged systems, the calculated lattice parameter, bulk modulus, and magnetic moments are in excellent agreement with the experimental values.

Keywords : first-principles calculation, FLAPW method, convergence, explicit orthogonalization (XO), ferromagnetism, bcc Fe

1. Introduction

First-principles calculations based on density functional theory (DFT) [1], although are non-trivial, have grown into an important method for describing materials in condensed matter physics, chemistry, and materials science. DFT can give detailed predictions of the atomic, electronic, and magnetic properties of materials and so, combined with the corresponding experiments, has become a powerful tool [2].

The augmented plane-wave (APW) method [3] was the first approach to combine atomic-like functions and a plane-wave basis set in order to automatically satisfy the Bloch symmetry on the one hand and to avoid the difficulties of the Wigner-Seitz cellular method [4] on the Wigner-Seitz cell boundary on the other. Korringa, Kohn, and Rostoker [5] suggested another modified method, the KKR method, to the Wigner-Seitz cellular method that employed phase-shifted spherical waves in the interstitial region instead of

the plane-waves of the APW method. The difficulty in the APW and KKR methods appears in the resulting secular matrix which depends non-linearly on energy. This difficulty was resolved by the introduction of the linearization of the APW and KKR basis sets, which developed to the linearized APW (LAPW) and the linearized muffin-tin orbital (LMTO) methods, respectively [6, 7]. Due to the flexibility and the accuracy of the linearization method, the full-potential linearized augmented plane-wave (FLAPW) method was developed to solve the total-energy problem in density functional theory for film [8, 9] and bulk [10] materials without any shape approximations on the valence electrons [11]. The FLAPW method is now considered to be one of the most precise methods for solving the electronic structure problems of crystalline solids.

The LAPW method for bulk systems separates space into two regions, the muffin-tin (MT) sphere region (non-overlapping atom centered spheres) and the remaining interstitial (I) region. The representation of the basis functions, charge densities, and potentials are different in the two regions. The basis functions in the method are given by

*Corresponding author: Tel: +82-54-279-9014
Fax: +82-54-279-9299, e-mail: igkim@postech.ac.kr

$$\chi(\mathbf{k}_n)= \begin{cases} \dfrac{1}{\sqrt{\Omega}}e^{i\mathbf{k}_n\cdot\mathbf{r}}, & \mathbf{r}\in\mathrm{I} \\[2ex] \Sigma_{l,m}[A^n_{lm}u_l(r,E_l)+B^n_{lm}\dot{u}_l(r,E_l)]\,Y_{lm}(\hat{\mathbf{r}}), & \mathbf{r}\in\mathrm{MT} \end{cases} \tag{1}$$

where $\mathbf{k}_n \equiv \mathbf{k} + \mathbf{K}_n$, $\mathbf{K}_n$ is a reciprocal lattice vector, Ω is the unit cell volume, u_l is solution of the (scalar relativistic) radial Schrödinger equation in the spherically averaged crystal potential at the linearization energy E_l, while $\dot{u}_l$ is the derivative with respect to around the energy parameter E_l. The coefficients A and B are determined by the condition that the basis functions are continuous and differentiable at the sphere boundary. There is a number of numerical cutoffs and parameters in the method: the number of plane waves in the basis set, determined by K_{max}; the MT radius R_{MT}; the angular momentum expansion l_{max} of the wave function in the sphere; and corresponding expansions parameters G_{max} and L_{max} for the charge and potentials. A crude rule of thumb [12] – related to the expansion properties of the plane wave – relates the l_{max} cutoff for the spherical harmonics to the K_{max} for the plane waves by $l_{max} = R_{MT}K_{max}$. While applying this relationship has the advantage of decreasing the number of independent parameters that needs to be chosen, it is important to note that, contrary to what might be inferred from common references [13], it does not guarantee convergence nor is it even necessarily a particularly good choice.

As seen in Table 1, which summarizes the convergence parameters collected mostly from the 21st century references [14-39], many FLAPW users have, in fact, adopted the convergence parameters of $l_{max} = R_{MT}K_{max} = 8$, a choice following from the work of Wei *et al.* [14], who found that the choice of the lattice harmonics construction with $L_{max} = 8$ was sufficient for bulk tungsten; these authors also used an angular momentum wave function cutoff of $l_{max} = 8$. However, Freeman *et al.* [15] used the convergence parameters $l_{max} = R_{MT}K_{max} = 10$ for simple cubic Fe.

In addition, there are many examples of the mismatch between l_{max} and $R_{MT}K_{max}$ as well [16-18, 20, 22, 23, 26, 27, 29-33, 38]. This diversity in the choice of convergence parameters is due in part to the lack of published systematic studies of the convergence parameters. In this paper, we examined the choice of convergence parameters which are widely used in the LAPW community. In Sec. 2, we briefly describe the method of convergence tests what we applied here. In Sec. 3, the numerical convergence of the FLAPW method are presented and discussed. Finally, a conclusion is given in Sec. 4.

2. Method for Convergence Test

The body-centered-cubic (bcc) bulk Fe of the experimental lattice constant of 5.4169 a.u. [40] was chosen as a representative system for the convergence test. Fe is located in the middle of the periodic table and shows ferromagnetism. Because of the combination of localized d-states and itinerant states, bcc Fe has long been considered a representative elemental material for testing first-principles and *ab initio* methods.

The Kohn-Sham equations [41] were solved using the FLAPW method. In order to check implementation dependence, we performed the calculation with two implementations of the FLAPW method; FLAIR [2] developed by the group of M. Weinert and the QMD-FLAPW package [42] developed by the group of A. J. Freeman. It is found that those two implementations give essentially the same results within numerical errors influenced by the different platform, i.e., the differences in the implemented numerical algorithms, the compilers (Intel FORTRAN or IBM XL FORTRAN), the central processing units (Intel or IBM POWER 5+), and the operating system (Linux or IBM AIX). Exchange-correlation was treated using the generalized gradient approximation (GGA) with the explicit form of Perdew, Burke, and Ernzerhof [43]. Core electrons were treated fully relativistically, while valence

Table 1. Collected references based on the choice of the convergence parameters in terms of $R_{MT}K_{max}$ and l_{max} of the FLAPW method on bulk systems.

$R_{MT}K_{max}$ \ l_{max}	7	8	9	10	11	12
6	–	[16]	–	–	–	–
7	–	[33]	–	[25, 26, 29]	–	–
8	[17]	[19, 21, 28] [34, 35, 37]	[23]	[22, 24, 27, 30, 31, 38]	–	[20]
9	–	[32, 39]	–	–	–	–
10	–	[18]	–	[15]	–	–
11	–	[18]	–	–	–	–
12	–	[18]	–	–	–	–

states were treated scalar relativistically, without spin-orbit coupling [44]. The explicit-orthogonalization (XO) scheme for ensuring the orthogonality between the semicore and valence states [2] was used throughout. Self-consistency was assumed when the charge density and the spin density differences were less than 10^{-5} electrons/a.u.^{3}

The star-function cutoff, G_{max}, which is used for describing the potential and density in the interstitial region, can be chosen in a number of ways. The valence density can be described strictly by a cutoff of $2K_{max}$, but because of both the solution of Poisson equation [11] and exchange-correlation, a larger value is required. In practice, for values $G_{max} \sim 3K_{max}$ or $G_{max} \sim 10$–15 $(2\pi/a)$, the results are rather insensitive to changes in G_{max}. Calculations using both a fixed $G_{max} = 15$ $(2\pi/a)$ and $G_{max} = 3K_{max}$ were done, with similar results.

Integrations inside the Brillouin zone (BZ) were performed by the improved tetrahedron method [45] on the $n \times n \times n$ Monkhorst-Pack mesh [46] with $3 \leq n \leq 21$, and

also by a special points integration scheme. The choice of the MT sphere radius of an element is often one of the most difficult and is a major focus here. Hence, we varied the MT sphere radius R_{MT} from 1.9 to 2.3 a.u. The plane-wave cutoff K_{max} was varied by considering the relation, $l_{max} = R_{MT}K_{max}$ for $6 \leq l_{max} \leq 12$, and also by independently varying K_{max}. The lattice constant of bcc Fe was optimized at each convergence parameter set by employing a seven-point least-square fit to the several standard equation of state [47-49], which also provides estimates of the bulk modulus (B).

3. Result and Discussion

Since the self-consistent solution of the Kohn-Sham equations is variational, i.e., gives an extremum of energy, we investigate the convergence of the total energy. In Fig. 1 the total energy for $R_{MT} = 1.9$ a.u. as a function of plane wave cutoff is shown for different l_{max}. Basically, the curves for the different l_{max} are indistinguishable, demonstrating that in fact there is no direct relationship between l_{max} and K_{max}. It is true, however, that as $R_{MT}K_{max}$ gets larger, l_{max} must increase otherwise the discontinuities of the basis functions become appreciable. A choice of $l_{max} = 8$–10 is generally a reasonable choice. The choice of the expansion for the charge and density should generally be that $L_{max} \geq l_{max}$, but this choice is not particularly critical.

In Fig. 2, we present the convergence behavior of the total energy for different MT radii, given both as a function of $R_{MT}K_{max}$ and K_{max}. In making comparisons the results of different R_{MT}, it is essential that the systems are treated as similarly as possible. An issue that needs special care is the treatment of the core states: They are not strictly confined to the MT spheres and to solve for them the potential must be extended beyond R_{MT}; in these plots, we apply the same algorithm for extending the potential beyond ~1.9 a.u. for each of the different R_{MT} values.

The overall convergence as a function of $R_{MT}K_{max}$ (in Fig. 2(b)) is similar for the different muffin-tin spheres, albeit the larger spheres converge somewhat faster. From this figure, using $R_{MT}K_{max}$ as a convergence parameter appears to be a reasonable choice, and a value around 10 gives good results. Note, however, that it is K_{max} that directly determines the size of the basis, and that for a given $R_{MT}K_{max}$, the ratio of the basis size for two different radii is $\sim(R_1/R_2)^3$; for example, the basis for $R_{MT} = 1.9$ a.u. is ~1.8 times as large as the one for $R_{MT} = 2.3$ a.u. This suggests that the convergence is better for the larger sphere, which is borne out by the upper plot which replots the data in terms of K_{max} (and hence the basis size)
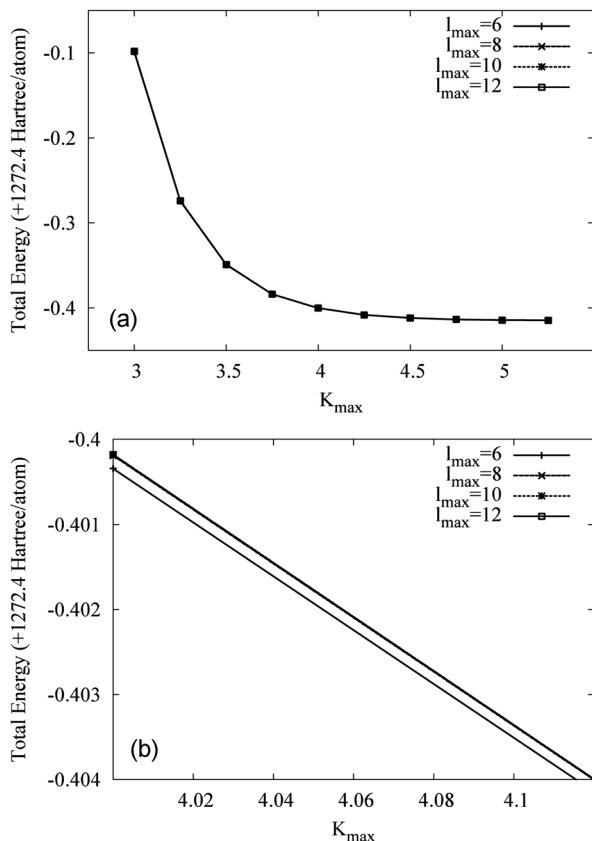

Fig. 1. (a) Convergence of the total energy as a function of K_{max} (in units of $2\pi/a$) for bcc Fe for $R_{MT} = 1.9$ a.u. for $l_{max} = 6$, 8, 10, and 12. Energies are given in Hartree/atom relative to the converged value. All the lines are overlapped into a single line. (b) The energies on an expanded scale. Note that the curves for $l_{max} = 8$, 10, and 12 still overlap on the mHartree/atom scale.
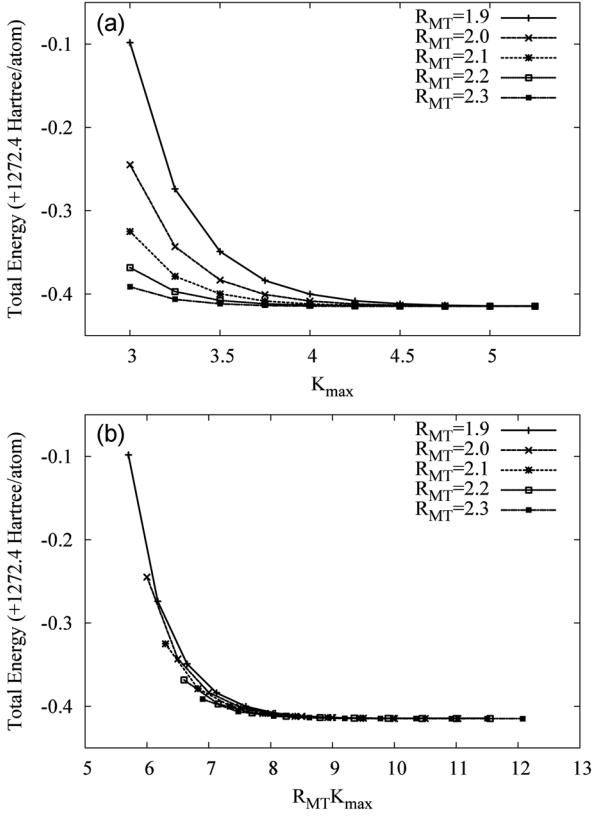
Fig. 2. Convergence of the total energy for bcc Fe for different MT radii R_{MT} as a function of (a) K_{max} (in units of $2\pi/a$) and (b) $R_{MT} K_{max}$. Energies are given in Hartree/atom relative to the converged value.

Table 2. Calculated number of core electrons outside the MT sphere of radius R_{MT} per spin (lost-core), the lowest eigenvalue Γ_1 of each spin relative to the Fermi energy, and the total energy. Energies are given in units Hartree. The lines marked "Δ" correspond to the changes in the quantities when the extrapolation for the core potential starts at R_{MT} rather than at 1.9 a.u.

R_{MT} (a.u.)	Lost Core ↑	Lost Core ↓	Eigenvalue Γ_1 ↑	Eigenvalue Γ_1 ↓	Total Energy (Hartree)
1.9	0.0434	0.0459	−0.30352	−0.29771	−1272.81433
Δ	–	–	–	–	0.00000
2.0	0.0299	0.0318	−0.30371	−0.29792	−1272.81453
Δ	−0.0009	−0.0007	−0.00033	−0.00031	0.00313
2.1	0.0205	0.0221	−0.30379	0.29801	−1272.81455
Δ	−0.0012	−0.0008	−0.00048	−0.00049	0.00455
2.2	0.0142	0.0154	−0.30380	−0.29801	−1272.81459
Δ	−0.0012	−0.0008	−0.00056	−0.00060	0.00537
2.3	0.0099	0.0107	−0.30372	−0.29794	−1272.81471
Δ	−0.0011	−0.0007	−0.00064	−0.00068	0.00602

directly. This behavior results from the fact that the optimally adapted numerical radial functions describe a larger fraction of the volume. In addition, use of K_{max} is a better idea of the computational cost-basis size and is applicable to systems composed of different atoms with intrinsically different atomic sizes.

In Table 2 we show the number of core electrons outside the MT sphere per spin, the corresponding lowest eigenvalue at Γ of each spin relative to the Fermi level, and the total energies for different R_{MT}. The charge lost from the core decreases rapidly with increasing R_{MT}. The positions of the lowest Γ_1 eigenvalues remain essentially constant, demonstrating that the converged calculated physical properties are essentially independent of the choice of R_{MT}. The total energy is slightly lower for the largest sphere, as expected if the numerical functions provide better variational freedom. The core leakage into the interstitial for smaller R_{MT} often leads to "ghost" states in the standard LAPW approach because the assumed orthogonality between the core and valence electrons breaks down. The XO approach [2] used here avoids that problem, as would so-called "local orbitals." Also shown (in

the lines labeled "Δ") are the changes that occur when the potentials for the core states are extended starting from R_{MT} as is usually done, and show how using different ("hidden") computational parameters need to be accounted for. As seen, there are systematic changes resulting from the subtle changes in the potential for the core states. The most noticeable effect is on the total energy, with changes large enough to be physically significant if naively taken at face value. This energy difference is due to changes mainly in the core eigenvalues because of the changed boundary conditions for the core states. The procedure used above avoids this issue, as would a frozen core approximation. However, the best, and most consistent, procedure that allows for meaningful comparisons among different calculations, is to simply pick a radius for each atom and use that set of radii in all the calculations.

In Table 3, we summarize the calculated static physical properties, i.e., equilibrium lattice parameter a (in units of a.u.) and bulk modulus B (in units of GPa), for the case of $K_{max} = 3.5$, 4, and 5 $(2\pi/a)$ and $R_{MT}K_{max} = 10$ for the BZ integration mesh of $17 \times 17 \times 17$ that the a and B values are converged well enough. Note that $K_{max} = 3.5$ $(2\pi/a)$ case is hardly to say it is converged. The calculated equilibrium lattice parameters for the $K_{max} = 5$ $(2\pi/a)$ or $R_{MT}K_{max} = 10$ are underestimated by less than 1% compared with the experimental value [40]. It is an excellent agreement with experiment if we consider the current calculation is for zero Kelvin, while the experimental value is obtained at a finite temperature.

We also found that the calculated B for $K_{max} = 4$ and 5 $(2\pi/a)$ or $R_{MT}K_{max} = 10$ results differs by a few percent

Table 3. Calculated static physical properties, equilibrium lattice parameter a (in units of a.u.) and bulk modulus B (in units of GPa), for the case of K_{max} = 3.5, 4, and 5 ($2\pi/a$) and $R_{MT}K_{max}$ = 10 and the BZ integration mesh of 17 × 17 × 17.

R_{MT} (a.u.)	K_{max} = 3.5		K_{max} = 4		K_{max} = 5		$R_{MT}K_{max}$ = 10	
	a	B	a	B	a	B	a	B
1.9	5.321	628.3	5.339	188.2	5.378	162.8	5.378	163.3
2.0	5.336	342.3	5.351	175.4	5.368	167.3	5.381	165.4
2.1	5.356	229.7	5.359	174.7	5.367	171.8	5.383	167.9
2.2	5.372	192.5	5.365	175.8	5.369	174.4	5.387	170.1
2.3	5.384	180.5	5.369	178.0	5.372	176.5	5.392	173.7
Theory (Ref. [47])	–	214.1						
Exp. (Ref. [41])	5.4169							
Exp. (Ref. [48])	–	173.1						

Table 4. Calculated total magnetic moments per atom μ_T and in the sphere μ_R (in units of μ_B) for different sphere radii.

R_{MT} (a.u.)	μ_T	μ_R
1.9	2.269	2.281
2.0	2.269	2.305
2.1	2.269	2.321
2.2	2.269	2.328
2.3	2.269	2.329

from the experimental one [51]. This is remarkable improvement compared to the previous results by Moruzzi and Marcus [50] using the augmented-spherical-wave (ASW) based on the local spin density approximation (LSDA). The bulk modulus is defined by

$$B = -V\frac{\partial P}{\partial V} = -V\frac{\partial}{\partial V}\left(\frac{\partial E}{\partial V}\right)_N = V\frac{\partial^2 E}{\partial V^2}, \qquad (2)$$

in the second derivative of energy with respect to volume [52]. This implies that the bulk modulus is an indication of the convexity of the total energy with respect to volume change of a system. Because any direct numerical derivative of any smooth function causes large roundoff errors [53], one should be careful in the procedure for obtaining B: The standard method is to calculate total energy at several lattice parameters to fit into a standard function of equation of states [47-49] and then perform the corresponding analytic derivative on it. Denser sampling points give better convergence in B calculation. A further contribution is the discrete nature of the reciprocal lattice: changes in lattice constant will cause different rings of **K** vectors to cross the K_{max} sphere, thereby changing the number of basis functions, an effect that is more significant for smaller K_{max}. This effect is also more pronounced for smaller BZ sampling meshes. However, the converged physical properties, i.e., ones that calculated with large enough basis functions give only a few percent difference as compared with experimental values [40, 51].

In Table 4, we present the calculated total magnetic
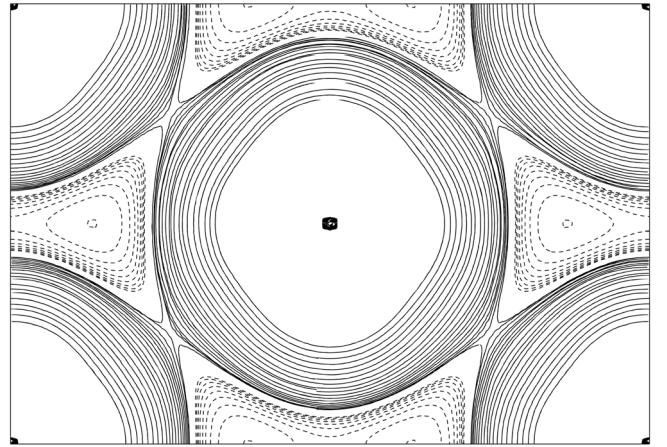
Fig. 3. Calculated spin density contour plot on the (110) plane of bcc Fe for the case of R_{MT} = 2.2 a.u., l_{max} = 10, and the BZ integration mesh of 17 × 17 × 17. Solid lines and broken lines represent the positively and negatively polarized spin densities, respectively. Contours start from ±1.0 × 10^{-3} electrons/a.u.^{3} and the subsequent contours are increased by a factor $\sqrt{2}$.

moments in the unit cell and in sphere. The total calculated magnetic moment is stable with respect to sphere size and is in excellent agreement with the experimentally known value [54]. On the other hand, μ in the sphere should depend on the volume occupied by the MT sphere in the unit cell. For ferromagnetic bcc Fe, the majority spins are concentrated around the atomic site. However, there are negative dog-bone shape regions in the interstitial region with minority spins, as seen in Fig. 3. As consequence, μ in the sphere first increases with R_{MT}, will decrease as the radius increases beyond 2.3 a.u.

4. Conclusion

We have tested the convergence behavior of the total energy for ferromagnetic bulk bcc Fe using the all-electron FLAPW method with the XO scheme. The dependence of the convergence on the star function cutoff G_{max}

is found to be minimal and a value around three times K_{max} of the plane-wave cutoff is reasonable. The customary relationship $l_{max} = R_{MT}K_{max}$, while a reasonable rule of thumb, is not justified in practice and a more reasonable approach is to check the convergence with respect to K_{max} directly. Likewise, the dependence on l_{max} was found to be small, and values of $l_{max} = 8$–10 are reasonable choices in a variety of cases. In general, to be able to compare total energies, it is important to keep as many computational parameters as possible constant; in particular, while the calculated properties are fairly insensitive to the choice of MT radii, using the same radius and mesh parameters will facilitate comparisons among different calculations. This is due to in part the power of the XO treatment on the basis functions.

For converged systems, the calculated lattice parameter and bulk modulus agree with the experimental values within a few percent difference by the theory. Similarly, the calculated magnetic moment is in excellent agreement with the experimental number. We found that the calculation of physical properties requires the careful consideration of the possible roundoff errors during the numerical derivatives. Thus, it is important to understand the convergence of calculated properties when trying to extract physical trends.

Acknowledgements

References

[1] P. Hohenberg and W. Kohn, Phys. Rev. **136**, B864 (1964).

[2] M. Weinert, G. Schneider, R. Podloucky, and J. Redinger, J. Phys.: Condens. Matter **21**, 084201 (2009).

[3] J. C. Slater, Phys. Rev. **51**, 846 (1937).

[4] E. Wigner and F. Seitz, Phys. Rev. **43**, 804 (1933); *ibid.* **46**, 509 (1934).

[5] J. Korringa, Physica **13**, 392 (1947); W. Kohn and N. Rostoker, Phys. Rev. **94**, 1111 (1954).

[6] D. D. Koelling and G. O. Arbman, J. Phys. F **5**, 2041 (1975).

[7] O. K. Andersen, Phys. Rev. B **12**, 3060 (1975).

[8] E. Wimmer, H. Krakauer, M. Weinert, and A. J. Freeman, Phys. Rev. B **24**, 864 (1981), and references therein.

[9] M. Weinert, E. Wimmer, and A. J. Freeman, Phys. Rev. B **26**, 4571 (1982).

[10] H. J. F. Jansen and A. J. Freeman, Phys. Rev. B **30**, 561 (1984).

[11] M. Weinert, J. Math. Phys. **22**, 2433 (1981).

[12] T. L. Loucks, *Augmented Plane Wave Method* (Benjamin, New York, 1967).

[13] D. Singh, Planewaves, *Pseudopotentials and the LAPW Method* (Kluwer Academic Publishers, Boston, 1994).

[14] S.-H. Wei, H. Krakauer, and M. Weinert, Phys. Rev. B **32**, 7792 (1985).

[15] A. J. Freeman, A. Continenza, S. Massidda, and J. C. Grossman, Physica C **166**, 317 (1990).

[16] S. Massidda, A. Continenza, A. J. Freeman, T. M. de Pascal, F. Meloni, and M. Serra, Phys. Rev. B **41**, 12709 (1990).

[17] H. Tanaka, H. Harima, T. Yamamoto, H. Katayama-Yoshida, Y. Nakata, and Y. Hirotsu, Phys. Rev. B **62**, 15042 (2000).

[18] C. Stamp, W. Mannstadt, R. Asahi, and A. J. Freeman, Phys. Rev. B **63**, 155106 (2001).

[19] W. T. Geng, A. J. Freeman, and G. B. Olson, Solid State Commun. **119**, 585 (2001).

[20] A. E. Merad, M. B. Kanoun, J. Cibert, H. Aourag, G. Merad, Mater. Chem. Phys. **82**, 471 (2003).

[21] S. Di Napoli, A. M. Llois, G. Bihlmayer and S. Blügel, M. Alouani, and H. Dreyssé, Phys. Rev. B **70**, 174418 (2004).

[22] A. D. Sayede, T. Amriou, M. Pernisek, B. Khelifa, and C. Mathieu, Chem. Phys. **316**, 72 (2005).

[23] K. Nakamura, T. Ito, and A. J. Freeman, Phys. Rev. B **72**, 064449 (2005).

[24] M. Sahnoun, C. Daul, M. Driz, J. C. Parlebas, and C. Demangeat, Comput. Mater. Sci. **33**, 175 (2005).

[25] R. Terki, G. Bertrand, H. Aourag, C. Coddet, Mater. Sci. in Semiconductor Processing **9**, 1006 (2006).

[26] V. Mishra, S. Chaturvedi, Physica B **393**, 278 (2007).

[27] A. V. Santos, Physica B **387**, 136 (2007).

[28] B. Białek and Jae Il Lee, J. Magnetics **12**, 93 (2007).

[29] T. Cai, H. Han, C. Zhang, J. Zhou, Y. Yu, and T. Gao, Solid State Commun. **146**, 368 (2008).

[30] N. I. Medvedeva and A. J. Freeman, Scripta Mater. **58**, 671 (2008).

[31] R. Miloua, Z. Kebbab, F. Miloua, and N. Benramdane, Phys. Lett. A **372**, 1910 (2008).

[32] Gul Rahman and In Gee Kim, J. Magnetics **13**, 124 (2008).

[33] S. J. Youn and S. C. Hong, J. Magnetics **13**, 140 (2008).

[34] W. S. Yun, Gi-Beom Cha, and S. C. Hong, J. Magnetics **13**, 144 (2008).

[35] Y. R. Jang and J. I. Lee, J. Magnetics **13**, 7 (2008).

[36] K. Nakamura, R. Shimabukuro, Y. Fujiwara, T. Akiyama, T. Ito, and A. J. Freeman. Phys. Rev. Lett. **102**, 187201 (2009).

[37] Gul Rahman, J. Magn. Magn. Mater. **321**, 2775 (2009).

[38] S. Drablia, H. Meradji, S. Ghemid, G. Nouet, and F. El Haj Hassan, Comput. Mater. Sci. **46**, 376 (2009).

[39] Jae Hoon Jang, In Gee Kim, and H. K. D. H. Bahdeshia, Comput. Mater. Sci. **44**, 1319 (2009).

[40] R. Kohlhaas, P. Donner, and N. Schmitz-Pranghe, Z. Angew. Phys. **23**, 245 (1967).

[41] W. Kohn and L. J. Sham, Phys. Rev. **140**, A1133 (1965).

[42] See http://www.flapw.com.

[43] J. P. Perdew, K. Burke, and M. Ernzerhof, Phys. Rev. Lett. **77**, 3865 (1996).

[44] D. D. Koelling and B. N. Harmon, J. Phys. C **10**, 3107 (1977).

[45] J. -H. Lee, T. Shishidou, and A. J. Freeman, Phys. Rev. B **66**, 233102 (2002).

[46] H. J. Monkhorst and J. D. Pack, Phys. Rev. B **13**, 5188 (1976).

[47] F. D. Murnaghan, Proc. Nat'l. Acad. Sci. U.S.A. **30**, 244 (1944); F. Birch, Phys. Rev. **71**, 809 (1947).

[48] P. Vinet, J. H. Rose, J. Ferrante, and J. R. Smith, J. Phys.: Condens. Matter **1**, 1941 (1989).

[49] J.-P. Poirier and A. Tarantola, Phys. Earth Planet. In. **109**, 1 (1998).

[50] V. L. Moruzzi and P. M. Marcus, in Handbook of Magnetic Materials, edited by K. H. J. Buschow (Elsevier, Amsterdam, 1993), Vol. 7.

[51] O. L. Andersen, in *Physical Acoustics*, edited by W. P. Mason (Academic, New York, 1965), Vol. III-B, pp. 77-95.

[52] N. W. Ashcroft and N. D. Mermin, *Solid State Physics* (Thomson Learning, Singapore, 1976) p. 39.

[53] W. H. Press, S. A. Teukolsky, W. T. Vetterling, and B. P. Flannery, *Numerical Recipies: The Art of Scientic Computing* 3rd edition (Cambridge University Press, Cambridge, 2007) Sec. 5.7.

[54] C. Kittel, *Introduction to Solid State Physics* 8-th edition (John-Wiley & Sons, International Editions, 2005) p. 328.